X-ray diffraction study on pressure-induced phase transformations and the equation of state of ZnGa2Te4

D. Errandonea, R. S. Kumar, O. Gomis, F. J. Manjón, V. V. Ursaki, and I. M. Tiginyanu

X-ray diffraction study on pressure-induced phase transformations and the equation of state of ZnGa$_2$Te$_4$

D. Errandonea,[1,a)] R. S. Kumar,[2] O. Gomis,[3] F. J. Manjón,[4] V. V. Ursaki,[5]
and I. M. Tiginyanu[5]

[1]*Departamento de Física Aplicada-ICMUV, MALTA Consolider Team, Universidad de Valencia, Edificio de Investigación, C/Dr. Moliner 50, Burjassot, 46100 Valencia, Spain*
[2]*High Pressure Science and Engineering Center, Department of Physics and Astronomy, University of Nevada Las Vegas, 4505 Maryland Parkway, Las Vegas, Nevada 89154-4002, USA*
[3]*Centro de Tecnologías Físicas: Acústica, Materiales y Astrofísica, MALTA Consolider Team, Universitat Politècnica de València, 46022 València, Spain*
[4]*Instituto de Diseño para la Fabricación y Producción Automatizada, MALTA Consolider Team, Universitat Politècnica de València, 46022 València, Spain*
[5]*Institute of Applied Physics, Academy of Sciences of Moldova, 2028 Chisinau, Moldova*

We report on high-pressure x-ray diffraction measurements up to 19.8 GPa in zinc digallium telluride (ZnGa$_2$Te$_4$) at room temperature. An irreversible structural phase transition takes place at pressures above 12.1 GPa and upon decompression a third polymorph of ZnGa$_2$Te$_4$ was recovered as a metastable phase at pressures below 2.9 GPa. Rietveld refinements were carried out for the three detected polymorphs, being their possible crystal structures reported. The axial compressibilities for the low-pressure phase of ZnGa$_2$Te$_4$ have been determined as well as the equation of state of the low- and high-pressure phases. The reported results are compared with those available in the literature for related compounds. Pressure-induced coordination changes and transition mechanisms are also discussed. © *2013 AIP Publishing LLC*. [http://dx.doi.org/10.1063/1.4851735]

I. INTRODUCTION

Defect-chalcopyrite (DC) and defect-stannite (DS) compounds are members of the adamantine-type AB$_2$X$_4$ family of semiconductors. These materials are currently being investigated due to their diversity of applications which include optoelectronics, non-linear optics, and electro-optics among others.[1] Zinc digallium telluride (ZnGa$_2$Te$_4$) is part of this family of compounds. It has been proposed as a promising material for developing phase-change memory devices.[2] To develop these potential applications, a correct determination of the electronic properties of ZnGa$_2$Te$_4$ is needed, for which a precise knowledge of its crystal structure is fundamental. This structure has been studied by x-ray diffraction (XRD)[3] and *ab initio* calculations.[4] According to previous experiments, ZnGa$_2$Te$_4$ crystallizes in the tetragonal DC structure (space group $I\bar{4}$), however, its structure has not been fully refined and its yet under debate being also the DS structure a good candidate for it (space group $I\bar{4}2m$).[5]

High-pressure (HP) structural studies on AB$_2$X$_4$ compounds have received increasing attention in the last years. Among other techniques, they have been studied by XRD, being several pressure-induced transitions reported.[6–15] The reversibility of these transitions is subject of dispute. In some cases, it has been found that the transitions are not reversible, being metastable polymorphs recovered at ambient conditions after decompression. These polymorphs have a smaller electronic band gap than the ambient-pressure stable polymorph,[16] opening the door to novel applications for

AB$_2$X$_4$ semiconductors. In contrast with other AB$_2$X$_4$ compounds, only few works have been devoted to the study of the structural properties of ZnGa$_2$Te$_4$[3,4] and no records of HP studies can be found in the literature. Here, we report room-temperature (RT) synchrotron HP XRD measurements up to 19.8 GPa to study into detail the structural properties of the low-pressure phase of ZnGa$_2$Te$_4$ and the possible occurrence of structural phase transitions. The RT equation of state (EOS) of the different polymorphs found in ZnGa$_2$Te$_4$ will be presented. Technical aspects of the experiments are described in Sec. II. Results are presented and discussed in Sec. III and conclusions are summarized in Sec. IV.

II. EXPERIMENTAL DETAILS

Single crystals of ZnGa$_2$Te$_4$ were grown by chemical vapor method using iodine as a transport agent.[17] The as-grown crystals of uniform dark-red color represent triangular prisms with mirror-like surfaces. Their chemical composition was verified by energy-dispersive x-ray analysis with a Phillips XL-30 scanning electron microscope. No impurities have been detected and the determined stoichiometry of the crystals corresponds to pure ZnGa$_2$Te$_4$ with a precision of 0.2%. Angle-dispersive XRD experiments were carried out at RT under pressure up to 19.8 GPa using a diamond-anvil cell (DAC) at Sector 16-IDB of the HPCAT, at the Advanced Photon Source (APS). Measurements were also carried out on decompression. Experiments were performed with an incident monochromatic wavelength (0.3681 Å). The sample used was a 10-μm thick pre-pressed pellet prepared using a finely ground powder obtained from the as grown single crystals. The pellet was loaded in a

a)Author to whom correspondence should be addressed. Electronic mail: daniel.errandonea@uv.es

130-μm hole of a 50-μm thick rhenium gasket in a DAC with diamond-culet sizes of 350 μm. Ruby grains were loaded with the sample for pressure calibration[18] and a 4:1 methanol-ethanol mixture was used as pressure-transmitting medium.[19,20] Pressure was assumed as the average of the pressure determined from different rubies and the accuracy assumed to be the standard deviation from average. In order to ensure the accuracy of the experiments, special attention was paid to avoiding the sample or the ruby grains bridging with the anvils. The x-ray beam was focused down to $10 \times 10 \ \mu m^2$ using Kirkpatrick-Baez mirrors. The images were collected using a MAR345 image plate located 380 mm away from the sample. The collected images were integrated and corrected for distortions using FIT2D.[21] The structure refinements were performed using the POWDERCELL[22] program package.

III. RESULTS AND DISCUSSION

A. Crystal structure at ambient conditions

Figure 1 shows an XRD pattern collected in $ZnGa_2Te_4$ at ambient pressure. It could be satisfactorily indexed with both the DC ($I\bar{4}$) or the DS ($I\bar{4}2m$) structures. Rietveld refinements considering both structures were carried out.
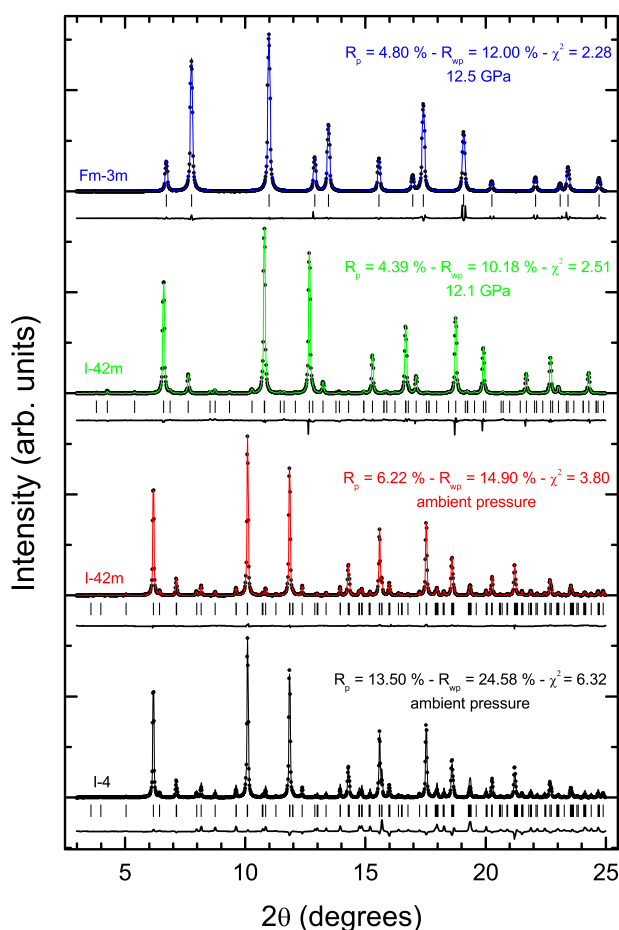

FIG. 1. RT XRD patterns of $ZnGa_2Te_4$ at selected pressures on upstroke. In all diagrams, the background was subtracted. The Rietveld refinements are also shown. Dots: experiments. Solid lines: calculated diffraction profiles and residuals. Calculated Bragg reflections are indicated with vertical ticks. R-factors and the χ^2 obtained from the refinements are also given.

The results of the Rietveld refinement obtained for both structures are shown in Fig. 1. In addition to the unit-cell parameters, we also refined the Te positions. The positions of Zn and Ga are fixed by the structural symmetry of both structures. Since the site occupancy factor (SOF) and the atomic displacement factors are correlated and more sensitive to background subtraction than positional parameters, the SOFs were constrained to the values given in Table I and the overall displacement factor, B, was fixed to 0.5 Å^2.[23] In this way, we reduced the number of free parameters used in the refinement. In the Rietveld analysis, we assumed as initial values for the Te coordinates those of Se in DS-$ZnGa_2Se_4$ (Ref. 9) and of S in DC-$CdGa_2S_4$ (Ref. 9). Table I provides the structural parameters obtained from the Rietveld refinements. As can be seen in Fig. 1, the results are more consistent with the DS structure on the basis of the refinement residuals. The parameters characterizing the goodness of fit (R-values and χ^2)[24] also support the assignment of the DS structure to the ambient conditions crystal structure of $ZnGa_2Te_4$. The refined structure agrees with the structure proposed by Hahn *et al.*,[5] who also assigned the space group $I\bar{4}2m$ to the structure of $ZnGa_2Te_4$. In contrast, our results contradict the conclusions of Rashmi and Dhawan[3] who assigned the space group $I\bar{4}$ to the same structure. On the other hand, our unit-cell parameters $a = 5.922(1)$ Å and $c = 11.809(2)$ Å are very similar to those previously reported.[3,5] The present results also correlate quite well with the structure calculated for DS $ZnGa_2Te_4$ using density-functional theory.[4] According with the refined structure, Ga atoms at the Wyckoff position 2a are four-coordinated by Te atoms, the bond distance being 2.627(4) Å. On the other hand, Ga and Zn atoms at the Wyckoff position 4d are four-coordinated by Te atoms, the bond distance being 2.617(4) Å.

B. Pressure-induced phase transitions

Upon compression, we did not observe any substantial change in the XRD patterns up to P > 12.1 GPa. In Fig. 1, it can be seen that the diffraction pattern can be still assigned to the tetragonal DS structure ($I\bar{4}2m$) at 12.1 GPa. The goodness of fit of the structural refinement with this model is similar at 12.1 GPa to that obtained at ambient pressure with the same model (see Fig. 1). Table II gives the structural parameters obtained from the Rietveld refinement at 12.1 GPa. By comparing Tables I and II, it can be seen that at 12.1 GPa the

TABLE I. Atomic positions and SOF of $ZnGa_2Te_4$ at ambient pressure. Top: DS structure ($I\bar{4}2m$, Z = 2). Bottom: DC structure ($I\bar{4}$, Z = 2). In both structures $a = 5.922(1)$ Å and $c = 11.809(2)$ Å.

Atom	Site	x	y	z	SOF
Ga	2a	0	0	0	1
Ga	4d	0	1/2	1/4	0.5
Zn	4d	0	1/2	1/4	0.5
Te	8i	0.2664(9)	0.2664(9)	0.1175(8)	1
Ga	2b	0	0	1/2	1
Ga	2c	0	1/2	1/4	1
Zn	2a	0	0	0	1
Te	8 g	0.2752(8)	0.2340(9)	0.1357(8)	1

TABLE II. Top: Atomic positions and SOF of DS-ZnGa$_2$Te$_4$ at 12.1 GPa ($I\bar{4}2m$, Z = 2). Bottom: same for DR-ZnGa$_2$Te$_4$ at 12.5 GPa ($Fm\bar{3}m$, Z = 1). In the DS structure $a = 5.532(1)$ Å and $c = 11.064(2)$ Å. In the DR structure $a = 5.432(2)$ Å.

Atom	Site	x	y	z	SOF
Ga	2a	0	0	0	1
Ga	4d	0	1/2	1/4	0.5
Zn	4d	0	1/2	1/4	0.5
Te	8i	0.2539(9)	0.2539(9)	0.1219(8)	1
Ga	4a	0	0	0	0.5
Zn	4a	0	0	0	0.25
Te	4b	1/2	1/2	1/2	1

ratio c/a is equal to 2 and the x and y coordinates of Te approaches the value 0.25 and the z coordinate approaches the value 0.125. Thus, pressure induces a symmetry increase of the crystal structure of ZnGa$_2$Te$_4$ so that it resembles a pseudo-rocksalt structure at 12.1 GPa with the *c*-axis doubled. At this pressure, the DS structure has Te atoms arranged in a similar fashion as in an fcc lattice and, similarly, Zn and Ga atoms also form an fcc lattice with one quarter of the atomic sites empty. The parameter of the cell of each of these fcc substructures of the DS phase is around 5.532 Å, being the distances between Te atoms and cations at 2a and 4d sites 2.402(5) Å and 2.415(5) Å, respectively. All the facts described above about the pressure-induced symmetry increase of ZnGa$_2$Te$_4$ have been also observed in ZnGa$_2$Se$_4$,[9] suggesting that they can be a common feature of DS compounds. In particular, in both compounds the displacement of the anions towards the position (0.25, 0.25, 0.125) and the increase of the axial ratio to reach $c/a = 2$ make the coordination tetrahedra in both compounds more regular. In special, the tetrahedral bond angles under compression approach all the ideal value of 109.5°. A meaningful explanation of the observed symmetry increase is beyond the scope of this work. However, a possible cause for it could be the fact that in ZnGa$_2$Te$_4$ and ZnGa$_2$Se$_4$ at ambient pressure the distance between anions is shorter along *c* than in the perpendicular axes. Thus, the opposite behavior is expected for the electrostatic repulsion among anions, making therefore the *c*-axis less compressible than the *a*-axis as found.

Upon further compression, at 12.3 GPa, we found the appearance of extra diffraction peaks, which indicates the onset of a structural phase transition. At 12.5 GPa, the new peaks fully develop and the peaks of the low-pressure phase cannot be detected anymore. As found in ZnGa$_2$Se$_4$ and related compounds,[8–13] we found that the XRD patterns of the HP structure of ZnGa$_2$Te$_4$ can be assigned to a cubic rocksalt-type structure ($Fm\bar{3}m$), where the Te atoms are located at the 4b site, while the Zn and Ga atoms are located at the 4a sites with a partial SOF. Results of the Rietveld refinements indicating the good match of this disordered rocksalt-type (DR) structure with the experimental results are shown in Fig. 1. Details of the structural model are given in Table II. We would like to stress here, that in spite the DR structure was previously assigned to the HP phase of other members of the AB$_2$X$_4$ family,[8–13] this is the first time that it

is assigned using enough Bragg peaks (fourteen) to be confident on the structural assignment. This was possible thanks to the large unit-cell volume of ZnGa$_2$Te$_4$ and the large angular aperture of the DAC used in the experiments ($2\theta < 25°$). The occurrence of the DS to DR transition, observed at P > 12.1 GPa, implies the completion of the symmetry increase that occurs in the low-pressure phase upon compression. Note that the unit-cell parameter of the cubic structure, $a = 5.432(2)$ Å, at 12.5 GPa implies an 1.7% contraction from the parameters defining the pseudo-rocksalt framework that can be drawn in the low-pressure tetragonal phase at 12.1 GPa. We have estimated a relative volume change per formula unit of −4.8% at 12.5 GPa, thus indicating that the DS to DR phase transition is a first-order transition. On the other hand, a comparison of the fcc sublattices of cations and anions in both DS and DR structures around 12 GPa (see Fig. 2) shows that a relative shift of the two fcc sublattices of the DS structure is needed (along the [111] direction or an equivalent one) in order that atoms of each fcc sublattice locate at the octahedral holes of the other
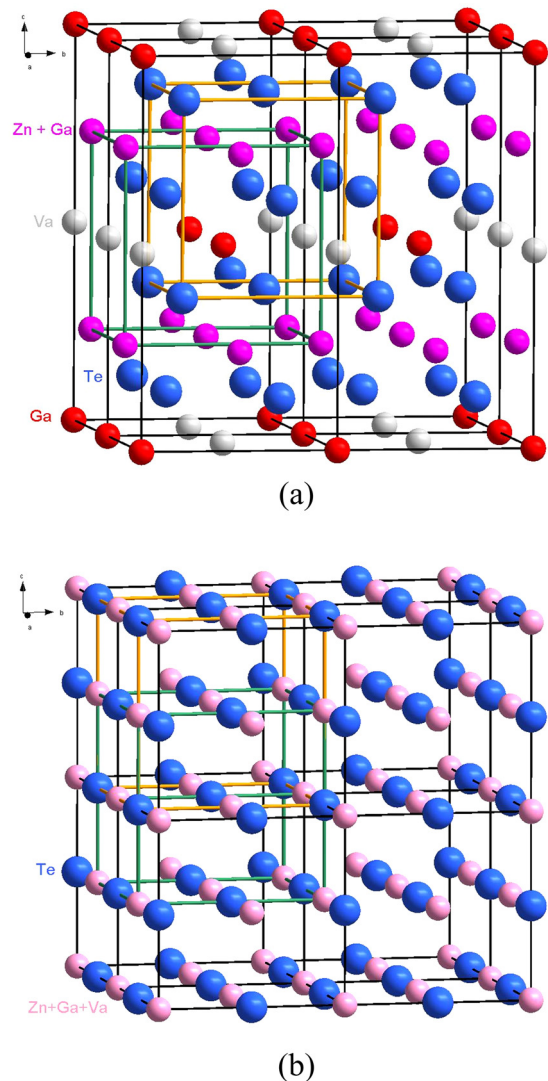

(a)

(b)

FIG. 2. Structure of DS-ZnGa$_2$Te$_4$ at 12.1 GPa (a) and of DR-ZnGa$_2$Te$_4$ at 12.5 GPa (b). For the sake of comparison, the cubic unit cells of the fcc-like sublattices of cations and anions in both structures are depicted in green and orange, respectively. Different atoms are identified in the figure.

sublattice, thus transforming the DS into the DR structure. The relative shift of the two fcc sublattices corresponds to the translation of Te atoms from tetrahedral voids to octahedral voids in the cation fcc sublattice. This fact suggests that the DS to DR transition might be a displacive transformation. Additionally, the described transition comprises a change in the coordination of both cations and anions from tetrahedral to octahedral, whose consequence is an increase of the cation-Te distance to 2.719(4) Å at 12.5 GPa in the DR phase compared to the that in the DS phase at 12.1 GPa whose average is 2.411 Å.

The DR phase remains stable up to the highest pressure reached in the experiments (19.8 GPa) as it is evidenced by the Rietveld refinement of the XRD pattern at this pressure to the DR phase shown at the bottom of Fig. 3 (residuals are small, and the R-factors and χ^2 indicate a good fit). Upon decompression, the DR structure is retained down to 2.9 GPa. In Fig. 3, we show how the XRD pattern measured at this pressure can be satisfactorily fitted with the same DR structure. However, after a subsequent decompression step in which we reached ambient pressure we observed an XRD pattern that cannot be explained either by the DS or the DR structures of $ZnGa_2Te_4$ (see Fig. 3). The irreversibility of the phase transition was already observed in other related AB_2X_4 compounds[8,10,11,13,25] and it was proposed that the recovered samples transformed to a metastable disordered zincblende-type (DZ) structure ($F\bar{4}3m$) at ambient

pressure.[8,10,11,13] In our case, we have been able to successfully reproduce the diffraction patterns collected at ambient pressure after decompression by assuming the DZ structure. Residuals and parameters indicating the quality of the structural refinement are given in Fig. 3 while the parameters of the refined structure are given in Table III. We would also like to mention here that during the structural refinement of the pattern at ambient pressure we obtained a decrease of the residuals of the structural refinement and consequently a better fit by reducing the symmetry of the DZ structure to the tetragonal subgroup ($I\bar{4}m2$) of the $F\bar{4}3m$ structure (see Fig. 3). Details of this tetragonal structure are given in Table III. Note that this structure reduces to the zincblende structure if $c/a = \sqrt{2}$, which is close to the axial ratio we obtain for the tetragonal structure (1.407). The small variation of c/a from $\sqrt{2}$ cause a subtle splitting of many Bragg peaks and therefore the tetragonal structure accounts better for the width of the diffraction peaks. However, the width of the peaks can be also explained by other factors like presence of defects in the sample, micro-strains and grain size.[26] Therefore, on the basis of the reported results we can only state that decompression of $ZnGa_2Te_4$ from the DR structure results in a metastable phase at ambient pressure whose structure is related to the DZ structure previously proposed for related compounds.[8,10,11,13,25] The crystal structure cannot be fully solved from HP powder XRD experiments and the accurate solution of the crystal structure of the recovered sample may probably need the performance of HP single-crystal experiments.[27]
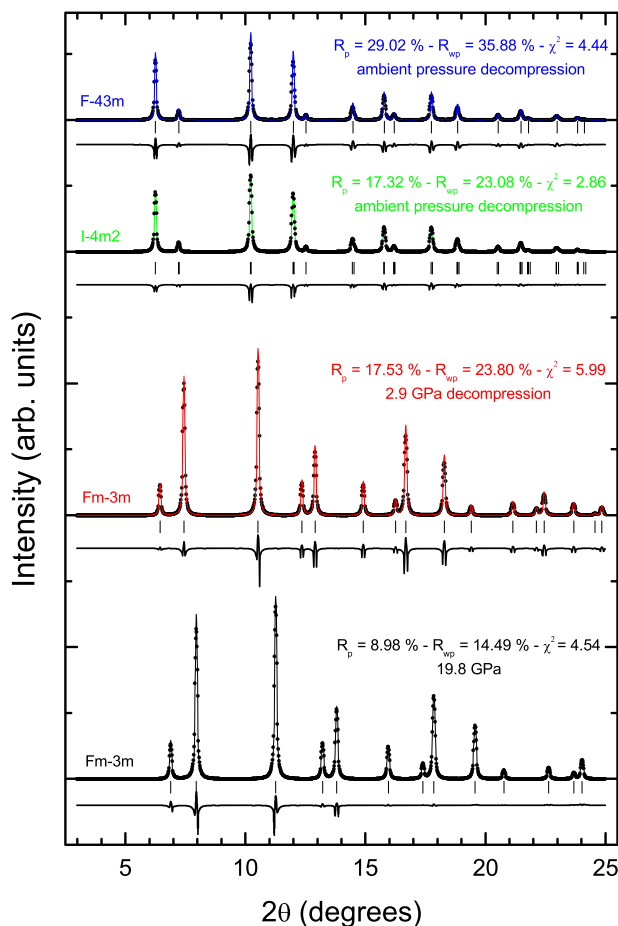
C. Room-temperature equation of state of the DS and DR phases

The pressure evolution of the unit-cell parameters of the low-(DS) and high-pressure (DR) phases has been obtained from the structural refinements. Results are listed in Tables IV and V. Figure 4 shows the pressure dependence of a and c for DS-$ZnGa_2Te_4$. The axial compressibilities at zero pressure $\left(\kappa_x = -\frac{\partial \ln x}{\partial P}\right)$ obtained by fitting of a Murnaghan EOS[28] are $\kappa_a = 8.48(6) \times 10^{-3}\,GPa^{-1}$, $\kappa_c = 8.09(7) \times 10^{-3}\,GPa^{-1}$; i.e., the c-axis is $\sim$5% less compressible than the a-axis. This fact is illustrated in the inset of Fig. 4 where we show the pressure dependence of the c/a ratio. As commented above, this ratio gradually increases from 1.994 at ambient pressure to 2 at 12.1 GPa.

FIG. 3. Same as Fig. 1 but showing XRD patterns collected on downstroke.

TABLE III. Top: Atomic positions and SOF of DZ-$ZnGa_2Te_4$ at ambient pressure ($F\bar{4}3m$, Z = 1). Bottom: same for proposed metastable tetragonal structure of $ZnGa_2Te_4$ at ambient pressure ($I\bar{4}m2$, Z = 1/2). In the DZ structure $a = 5.843(6)$ Å. In the tetragonal structure $a = 4.139(5)$ Å and $c = 5.823(5)$ Å.

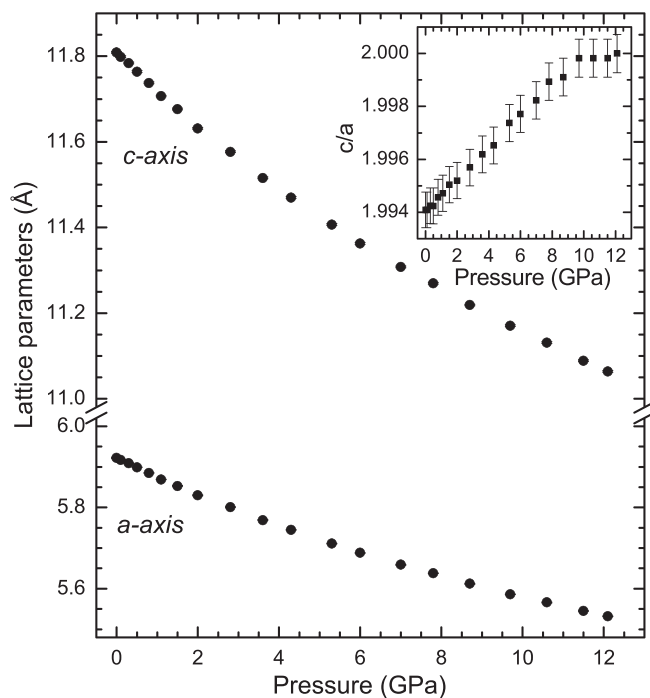| Atom	Site	x	y	z	SOF
Ga	4a	0	0	0	0.5
Zn	4a	0	0	0	0.25
Te	4c	1/4	1/4	1/4	1
Ga	2a	0	0	0	0.5
Zn	2a	0	0	0	0.25
Te	2c	0	1/2	1/4	1

TABLE IV. Experimental pressure (P), unit-cell parameters (a, c) and volume (V) of DS-ZnGa$_2$Te$_4$ with their standard deviations (esd).

P GPa	esd (P) GPa	a Å	esd (a) Å	c Å	esd (c) Å	V Å^3	esd (V) Å^3
0.00	0.02	5.922	0.001	11.809	0.002	414.14	0.21
0.10	0.02	5.917	0.001	11.799	0.002	413.09	0.21
0.30	0.02	5.909	0.001	11.784	0.002	411.45	0.21
0.50	0.02	5.899	0.001	11.764	0.002	409.37	0.21
0.80	0.02	5.885	0.001	11.738	0.002	406.52	0.21
1.10	0.02	5.869	0.001	11.707	0.002	403.25	0.21
1.50	0.02	5.853	0.001	11.677	0.002	400.03	0.21
2.00	0.02	5.830	0.001	11.632	0.002	395.36	0.20
2.80	0.02	5.801	0.001	11.577	0.002	389.58	0.20
3.60	0.02	5.769	0.001	11.516	0.002	383.27	0.20
4.30	0.02	5.745	0.001	11.470	0.002	378.57	0.20
5.30	0.02	5.711	0.001	11.407	0.002	372.05	0.20
6.00	0.02	5.688	0.001	11.363	0.002	367.63	0.19
7.00	0.02	5.659	0.001	11.308	0.002	362.13	0.19
7.80	0.02	5.638	0.001	11.270	0.002	358.24	0.19
8.70	0.02	5.612	0.001	11.219	0.002	353.34	0.19
9.70	0.02	5.586	0.001	11.171	0.002	348.57	0.19
10.60	0.04	5.566	0.001	11.131	0.002	344.84	0.19
11.50	0.04	5.545	0.001	11.089	0.002	340.95	0.18
12.10	0.04	5.532	0.001	11.064	0.002	338.59	0.18

FIG. 4. Pressure evolution of unit-cell parameters in DS-ZnGa$_2$Te$_4$. The inset shows the pressure evolution of the c/a ratio. Where not shown, error bars are smaller than symbols size.

Figure 5 shows the pressure dependence of the volume for the DS and DR phases. EOS parameters for both phases were determined by least-squares fits of 2nd (BM2) and 3rd (BM3) order Birch–Murnaghan EOSs[29] to the pressure-volume (P-V) data. Weights derived from the experimental uncertainties, in both pressure and volume, were assigned to each data point in the fits. They were carried out with the EoSFit software (v5.2).[30] Table VI summarizes the zero-pressure values of the volume (V$_0$), bulk modulus (B$_0$), and its pressure derivative (B$_0'$) obtained from the fits of both DS and DR phases. The obtained values for the weighted chi-squared, χ^2_w, are also given in the table. For both DS and DR phases, we found that the fit does not improve by leaving B$_0'$ as a free parameter. This result indicates that a 3rd order expansion of the EOS is not required to fit our experimental

data. In Fig. 5, it can be seen that both BM2 and BM3 fits accurately reproduce the experimental results. According to our results DS-ZnGa$_2$Te$_4$ is one of the compounds of the adamantine-type AB$_2$X$_4$ family with the smallest bulk modulus.[15] The bulk modulus of DR-ZnGa$_2$Te$_4$ is ~20% larger than that of the low-pressure phase, which is consistent with the volume collapse observed at the transition (see Fig. 5). In particular, the DR phase has a volume 4.8% smaller than the DS phase at 12.5 GPa as previously commented. In addition, if we compare the normalized volumes of the DS, DR, and
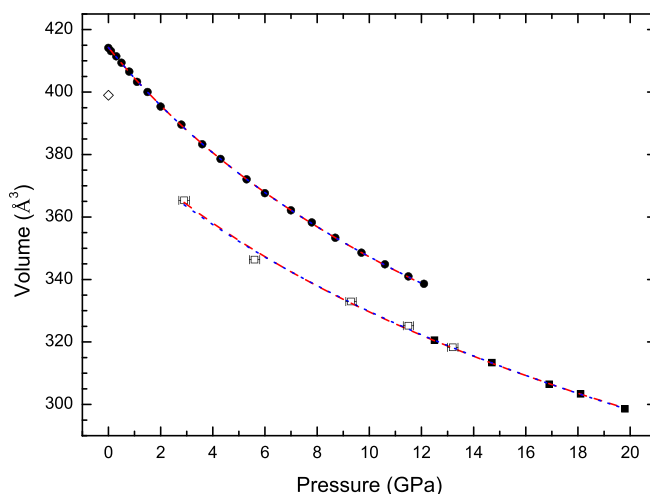
TABLE V. Experimental pressure (P), unit-cell parameters (a) and volume (V) of DR- ZnGa$_2$Te$_4$ with their standard deviations (esd). Last column indicates whether the measurement was done on compression or decompression.

P GPa	esd (P) GPa	a Å	esd (a) Å	V Å^3	esd (V) Å^3	Measurement
12.50	0.04	5.432	0.002	160.28	0.18	Upstroke
14.70	0.04	5.391	0.002	156.68	0.17	Upstroke
16.90	0.04	5.351	0.002	153.22	0.17	Upstroke
18.10	0.04	5.333	0.002	151.68	0.17	Upstroke
19.80	0.04	5.305	0.002	149.30	0.17	Upstroke
13.2	0.2	5.419	0.002	159.13	0.18	Downstroke
11.5	0.2	5.458	0.002	162.59	0.18	Downstroke
9.3	0.2	5.501	0.002	166.47	0.18	Downstroke
5.6	0.2	5.574	0.002	173.18	0.19	Downstroke
2.9	0.2	5.674	0.002	182.67	0.19	Downstroke

FIG. 5. Pressure evolution of unit-cell volume for different phases of ZnGa$_2$Te$_4$: Circles (DS), squares (DR), and diamond (DZ-like). To facilitate comparison for the three phases we have plotted the double of the unit-cell volume for DR and DZ phases. Solid (empty) symbols represent data measured on compression (decompression). Where not shown error bars are smaller than symbol size. The red dashed (blue dotted) lines represent 2nd (3rd) order BM EOSs.

TABLE VI. EOS parameters and χ^2_w for low- (DS) and high-pressure (DR) phases of $ZnGa_2Te_4$. Last two columns indicate the EOS type used and the maximum pressure deviation in absolute value ($|\Delta P|$) between the EOS and the experiment.

Phase	V_0 [Å³]	B_0 [GPa]	B_0'	χ^2_w	EOS	$|\Delta P|$ [GPa]
DS	414.3(1)	39.8(1)	4 (fixed)	0.64	BM2	0.064
DS	414.3(1)	39.7(5)	4.0(1)	0.68	BM3	0.063
DR	192.8(8)	47(1)	4 (fixed)	1.46	BM2	0.591
DR	192(1)	50(5)	3.7(4)	1.54	BM3	0.572

DZ phases at ambient pressure it is found that the volume of the DZ phase [399.0(1.2) Å³] is between those of the DS [414.14(21) Å³] and DR [385.6(1.6) Å³] phases. In the comparison, the volume for the DR phase at ambient pressure has been obtained from the BM2 EOS, and in the cases of the DR and DZ phases, volume was normalized multiplying by two. The volume of the three phases decreases in the sequence DS > DZ > DR which suggest that the compressibility of the DZ structure should be in between those of the other two phases since the packing efficiency of DZ is in between those of DS and DR.

In order to obtain a direct indication of the compressional behavior of DS-$ZnGa_2Te_4$ and of the quality of the EOS fit, the P–V data are transformed into F_E–f_E data where F_E (f_E) is the normalized stress (finite strain).[30] The same analysis cannot be done for DR-$ZnGa_2Te_4$ because its zero-pressure volume cannot be measured since the DR phase is not recovered at ambient pressure. The F_E–f_E plot for DS-$ZnGa_2Te_4$ (see Fig. 6) shows that data points lie on near a horizontal line of constant F_E corresponding to $B_0' = 4$.[30] In Fig. 6 it can be seen that a linear fit (dashed blue line) to F_E–f_E data gives a straight line almost parallel to the case when $B_0' = 4$ (solid red line). This result indicates that experimental data can be fitted with a BM2, thus
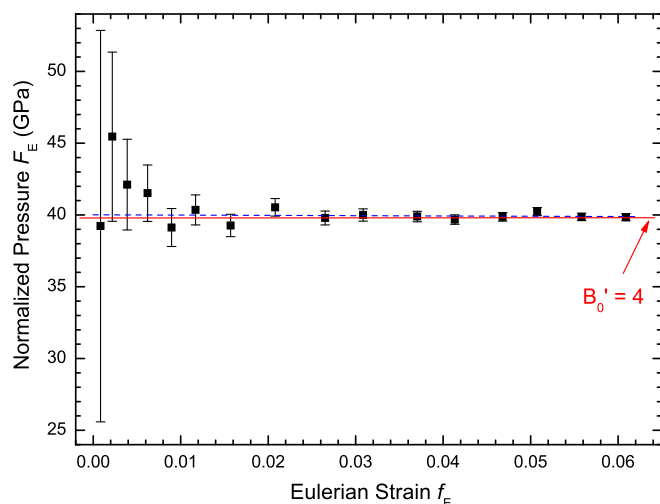
confirming the validity of the 2nd order EOS for the measured data. Moreover, a value of $B_0 = 40.0(3)$ GPa and $B_0' = 4.0(1)$ is obtained from the linear fit. In summary, these results confirm that the BM2 EOS is an adequate representation of the P-V data of DS-$ZnGa_2Te_4$ as previously found on the basis of statistical results from the EOS fits.

IV. CONCLUDING REMARKS

$ZnGa_2Te_4$ has been studied at RT using HP XRD up to 19.8 GPa. An irreversible phase transition has been detected at P > 12.1 GPa and a third polymorph of $ZnGa_2Te_4$ has been recovered as a metastable phase at ambient pressure. The crystal structure of the three observed polymorphs have been refined and discussed. The low-pressure phase has a defect stannite structure and the high-pressure phase a disordered rocksalt structure. The recovered metastable phase is consistent with a disordered zincblende structure or a subgroup of it. Finally, the axial compressibility of the low-pressure phase, and the RT P-V EOS of the low- and high-pressure phases are reported.

ACKNOWLEDGMENTS

FIG. 6. Volume–pressure data of DS-$ZnGa_2Te_4$ displayed as a plot of the normalized pressure F_E against the Eulerian strain f_E. The blue dashed line is a linear fit to experimental F_E–f_E data. The solid red line represents the case of a BM2 EOS with $B_0' = 4$.

[1]S. S. Fouad, G. B. Sakr, I. S. Yahia, and D. M. Abdel Basset, Mater. Res. Bull. **46**, 2141 (2011) and references therein.
[2]G. B. Sakr, S. S. Fouad, I. S. Yahia, and D. M. Abdel Basset, J. Mater. Sci. **48**, 1134 (2013).
[3]Rashmi and U. Dhawan, Powder Diffr. **17**, 41 (2002).
[4]J. Xiao-Shu, Y. Ying-Ce, Y. Shi-Min, M. Shu, N. Zhen-Guo, and L. Jiu-Qing, Chin. Phys. B **19**, 107104 (2010).
[5]H. Hahn, G. Frank, W. Klinger, A. D. Störger, and G. Störger, Z. Anorg. Allg. Chem. **279**, 241 (1955).
[6]O. Gomis, R. Vilaplana, F. J. Manjón, D. Santamaría-Perez, D. Errandonea, E. Pérez-González, J. López-Solano, P. Rodríguez-Hernández, A. Muñoz, I. M. Tiginyanu, and V. V. Ursaki, J. Appl. Phys. **113**, 073510 (2013).
[7]D. Santamaría-Pérez, M. Amboage, F. J. Manjón, D. Errandonea, A. Muñoz, P. Rodríguez-Hernández, A. Mujica, S. Radescu, V. V. Ursaki, and I. M. Tiginyanu, J. Phys. Chem. C **116**, 14078 (2012).
[8]S. Meenakshi, V. Vijyakumar, A. Eifler, and H. D. Hochheimer, J. Phys. Chem. Solids **71**, 832 (2010).
[9]D. Errandonea, R. S. Kumar, F. J. Manjón, V. V. Ursaki, and I. M. Tiginyanu, J. Appl. Phys. **104**, 063524 (2008).
[10]A. Grzechnik, V. V. Ursaki, K. Syassen, I. Loa, I. M. Tiginyanu, and M. Handfland, J. Solid State Chem. **160**, 205 (2001).
[11]O. Gomis, R. Vilaplana, F. J. Manjón, D. Santamaría-Pérez, D. Errandonea, E. Pérez-González, J. López-Solano, P. Rodríguez-Hernández, A. Muñoz, I. M. Tiginyanu, and V. V. Ursaki, Mater. Res. Bull. **48**, 2128 (2013).
[12]J. Marquina, Ch. Power, P. Grima, M. Morocoima, M. Quintero, B. Couzinet, J. C. Chervin, P. Munsch, and J. González, J. Appl. Phys. **100**, 093513 (2006).

[13]S. Meenakshi, V. Vijyakumar, B. K. Godwal, A. Eifler, I. Orgzall, S. Tkachev, and H. D. Hochheimer, J. Phys. Chem. Solids **67**, 1660 (2006).

[14]D. Errandonea, R. S. Kumar, F. J. Manjón, V. V. Ursaki, and E. V. Rusu, Phys. Rev. B **79**, 024103 (2009).

[15]O. Gomis, D. Santamaría-Pérez, R. Vilaplana, R. Luna, J. A. Sans, F. J. Manjón, D. Errandonea, E. Pérez-González, P. Rodríguez-Hernández, A. Muñoz, I. M. Tiginyanu, and V. V. Ursaki, J. Alloys Compd. **583**, 70 (2014).

[16]O. Gomis, R. Vilaplana, F. J. Manjón, E. Pérez-González, J. López-Solano, P. Rodríguez-Hernández, A. Muñoz, D. Errandonea, J. Ruiz-Fuertes, A. Segura, D. Santamaría-Pérez, I. M. Tiginyanu, and V. V. Ursaki, J. Appl. Phys. **111**, 013518 (2012).

[17]I. M. Tiginyanu, N. A. Modovyan, and O. D. Stoika, Sov. Phys. Solid State **43**, 527 (1992).

[18]H. K. Mao, J. Xu, and P. M. Bell, J. Geophys. Res. **91**, 4673, doi:10.1029/JB091iB05p04673 (1986).

[19]S. Klotz, J. C. Chervin, P. Munsch, and G. Le Marchand, J. Phys. D **42**, 075413 (2009).

[20]D. Errandonea, Y. Meng, M. Somayazulu, and D. Häusermann, Physica B **355**, 116 (2005).

[21]A. P. Hammersley, S. O. Svensson, M. Hanfland, A. N. Fitch, and D. Häusermann, High Press. Res. **14**, 235 (1996).

[22]W. Kraus and G. Nolze, J. Appl. Crystallogr. **29**, 301 (1996).

[23]O. Gomis, J. A. Sans, R. Lacomba-Perales, D. Errandonea, Y. Meng, J. C. Chervin, and A. Polian, Phys. Rev. B **86**, 054121 (2012).

[24]B. H. Tobby, Powder Diffr. **21**, 67 (2006).

[25]R. Vilaplana, O. Gomis, F. J. Manjón, H. M. Ortiz, E. Pérez-González, J. López-Solano, P. Rodríguez-Hernández, A. Muñoz, D. Errandonea, V. V. Ursaki, and I. M. Tiginyanu, J. Phys. Chem. C **117**, 15773 (2013).

[26]R. T. Downs and A. K. Singh, J. Phys. Chem. Solids **67**, 1995 (2006).

[27]J. Ruiz-Fuertes, A. Friedrich, J. Pellicer-Porres, D. Errandonea, A. Segura, W. Morgenroth, E. Haussühl, C.-Y. Tu, and A. Polian, Chem. Mater. **23**, 4220 (2011).

[28]M. D. Frogley, J. L. Sly, and D. J. Dunstan, Phys. Rev. B **58**, 12579 (1998).

[29]F. Birch, J. Geophys. Res. **83**, 1257, doi:10.1029/JB083iB03p01257 (1978).

[30]R. J. Angel, "Equations of state," in *High-Pressure and High-Temperature Crystal Chemistry*, edited by R. M. Hazen, R. T. Downs, MSA Reviews in Mineralogy and Geochemistry, vol. 41 (2000), pp. 35–60.